SAND2018-1697J

Phase conjugate digital inline holography (PCDIH)

DANIEL R. GUILDENBECHER,[1,*] KATHRYN N. GABET HOFFMEISTER,[1] W. MARLEY KUNZLER,[1] DANIEL R. RICHARDSON,[1] SEAN P. KEARNEY[2]

[1]*Engineering Sciences Center, Sandia National Laboratories, PO Box 5800, Mail Stop 0840, Albuquerque, NM 87185*
[2]*Spectral Energies LLC, 4065 Executive Drive, Dayton, OH 45430*
**Corresponding author: drguild@sandia.gov*

Received XX Month XXXX; revised XX Month, XXXX; accepted XX Month XXXX; posted XX Month XXXX (Doc. ID XXXXX); published XX Month XXXX

Digital inline holography (DIH) provides instantaneous three-dimensional (3D) measurements of diffracting objects; however, phase disturbances in the beam path can distort the imaging. In this letter, a phase conjugate digital inline holography (PCDIH) configuration is proposed for removal of phase disturbances. Brillouin enhanced four-wave mixing produces a phase conjugate signal which back propagates along the DIH beam path. Results demonstrate removal of distortions caused by gas-phase shocks to recover 3D images of diffracting objects. © 2017 Optical Society of America

OCIS codes: *(090.1995) Digital holography; (190.5040) Phase conjugation; (100.6890) Three-dimensional image processing.*

http://dx.doi.org/10.1364/OL.99.099999

Digital inline holography (DIH) has been widely applied for tracking and sizing of particles in three dimensions (3D) [1-4]. For example, Fig 1 shows DIH results from hypervelocity metal fragments generated by a laboratory-scale detonation [4]. In the experiment, a collimated laser beam propagates through the particle field resulting in diffraction patterns, which are recorded as a hologram (Fig 1a). After an experiment, this is numerically refocused via the diffraction-integral equation to reveal in-focus particle images at their original optical depths (Fig 1b). With appropriate processing routines [2, 3], particle sizes and 3D positions can be determined. Furthermore, digital sensors can be used for temporal resolution and 3D velocimetry [2, 4].

Advantages of DIH include the ability to perform 3D imaging with short-duration (<100 ns) laser pulses that freeze motion, limited optical access requirements along a single line of sight, and relatively long stand-off distances for equipment protection in hazardous environments [2, 4]. However, DIH is susceptible to image degradation due to phase disturbances from features in the flow field. This is illustrated in Fig 1 where the shock-waves from the leading fragments obscure downstream particles. Here, a phase conjugate digital inline holography (PCDIH) configuration is proposed and shown to remove such phase disturbances, while maintaining the ability to perform 3D imaging of absorptive objects.

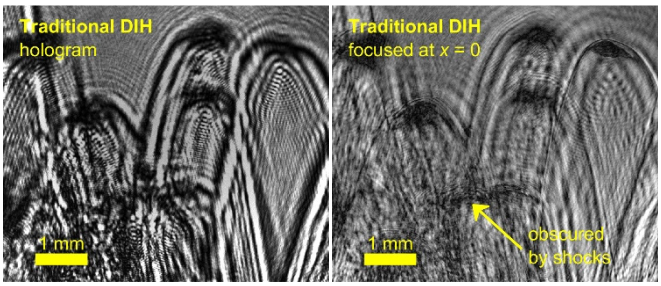

(a) (b)

Fig. 1. (a) Hologram of hypervelocity particles traveling from bottom to top and (b) results after numerical refocusing to the optical depth of the particle on the top right. Experimental details are available in [4].

A phase conjugate (PC) mirror produces a backward propagating beam with phase that is equal and opposite to the incoming beam [5, 6]. As demonstrated previously (e.g. [7-9]), a phase distortion placed in the incoming beam is canceled by the conjugate phase of the return beam resulting in optically restored imaging. This has been applied to analog holography where a hologram was first formed through an inhomogeneous glass plate and recorded on film. After development, reconstruction using the conjugate of the reference wave produced a PC object wave and a corrected image when viewed through the same glass plate [7]. Unfortunately, this method and related alternatives such as adaptive optics [10] are far too slow for correction of rapidly varying distortions, such as those shown in Fig 1. Instead, we propose four-wave mixing to generate a PC signal during the duration of a short-pulse laser (~60 ps in the current work). This is similar to previous imaging applications [8, 9] but to our knowledge has yet to be combined with holography.

The experimental setup is shown in Fig 2. A ~60 ps beam (Ekspla PL2231, 532 nm) is split into three legs. The first leg is spatially filtered and collimated before entering the left-hand side of the configuration in Fig 2. The beam passes through a 45° window, which has a single-side, 532 nm anti-reflective coating, such that ~5% of the incident light is reflected into a beam dump. The remainder passes through the measurement volume containing a stationary vertical wire (~200 μm diameter) at $x = 0$. Following this, a second single-side AR window reflects ~5% into a lens and camera (K2 long-distance microscope and LaVision sCMOS) forming a traditional digital inline hologram (DIH).

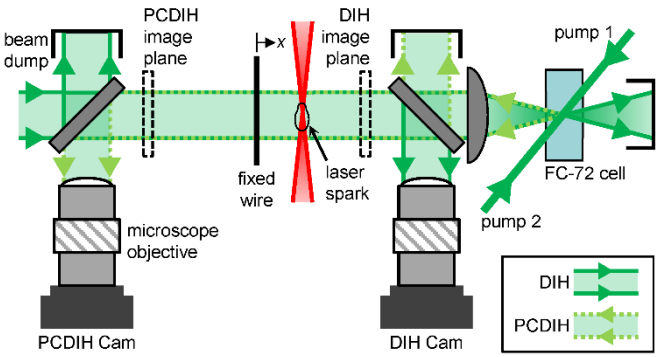

Fig. 2. Experimental configuration for simultaneous traditional DIH imaging (right camera) and PCDIH imaging (left camera) of a stationary object (wire) with index-of-refraction gradients along the beam path created by a laser-induced spark.

A PC signal is produced by focusing the remaining portion of the beam (~0.7 mJ) at ~f/10 into a cell containing a non-linear medium. Here, the heavy fluorocarbon FC-72 from 3M is utilized as a relatively safe alternative to other common liquids [11]. To achieve Brillouin-enhanced four-wave mixing (BEFWM), the two additional legs are arranged into counter-propagating pump beams as shown in Fig 2. Each pump beam is optically delayed such that all three beams arrive at the cell at the same instant. Pump beams are unfocused (~6 mm diameter) and ~4 mJ each. This arrangement produces a PC signal which back propagates along the image path as shown by the dotted light green lines in Fig 2. Approximately 5% of the PC signal is rejected by the window on the right while the remainder passes through the measurement volume. Finally, ~5% of this is reflected by the leftmost window into a second lens and camera (K2 long-distance microscope and LaVision sCMOS) forming the phase conjugate digital inline hologram (PCDIH).

The reflectivity of the BEFWM PC mirror is estimated by measuring the energy entering the PCDIH camera (~0.4 μJ at full pump energy) while accounting for the approximate beam splitting ratios of the single-side AR windows. Results are shown in Fig 3 as a function of varying pump energy. This plot indicates that the reflectivity is relatively low compared to some previous BEFWM work and is especially weak compared to alternative PC processes such as stimulated Brillouin scattering (SBS) [5]. If needed, future work could consider alternative configurations to both increase the PC signal and simplify the experimental arrangement. Nevertheless, as shown in the remainder of this work, the current signal to noise ratio is sufficient to achieve high-quality PCDIH images.

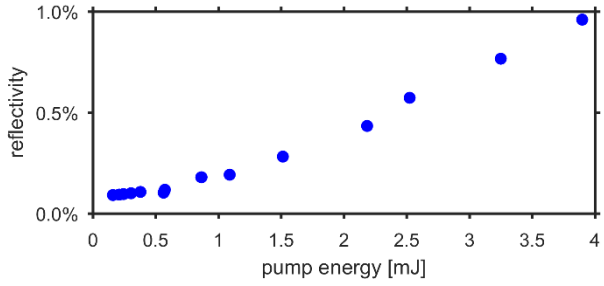

Fig. 3. Reflectivity of the phase conjugate (PC) mirror as a function of pump energy.

The configuration in Fig 2 allows for simultaneous PCDIH and traditional DIH imaging. Prior to an experiment, the magnification of the PCDIH and DIH cameras are adjusted to be identical to within 0.2%. In addition, the propagation distance between the fixed wire and the DIH image plane along the positive x-direction (61.2 mm) is closely matched to the distance between the wire and the PCDIH image plane along the negative x-direction (60.7 mm). Consequently, in absence of any phase disturbances, the PCDIH and DIH images are nearly identical. To study the corrective ability of the proposed PCDIH configuration, localized index-of-refraction gradients are created using a second laser (Continuum Surelite III, 1064 nm, 5 ns, ~400 mJ) focused at ~f/40 to create air breakdown and strong shocks. This is synchronized with the ps laser such that imaging is performed at ~400±200 ns after the laser spark.

Figure 4 shows experimental results when the laser spark is located at x = 15 mm. The top row shows the recorded PCDIH hologram on the left and traditional DIH hologram on the right. In the PCDIH image (top left) the large vertical diffraction patterns created by the wire as easily recognized. In contrast, in the normal DIH hologram (top right) the vertical diffraction patterns are clearly distorted due to the phase variations created by the laser spark. In the bottom row, these images are numerically refocused to x = 0. Dotted yellow lines show the measured apparent wire edges determined using the processing routines defined in [3]. In the PCDIH image (bottom left) an undistorted and in focus image of the vertical wire is obtained. On the other hand, in the traditional DIH image (bottom right) the wire appears highly distorted. Recall, this is an apparent distortion caused by the phase variations. In reality, the wire is fixed throughout the experiments. These results provide clear evidence that PCDIH can remove unwanted phase distortions to enable 3D imaging of absorptive objects.

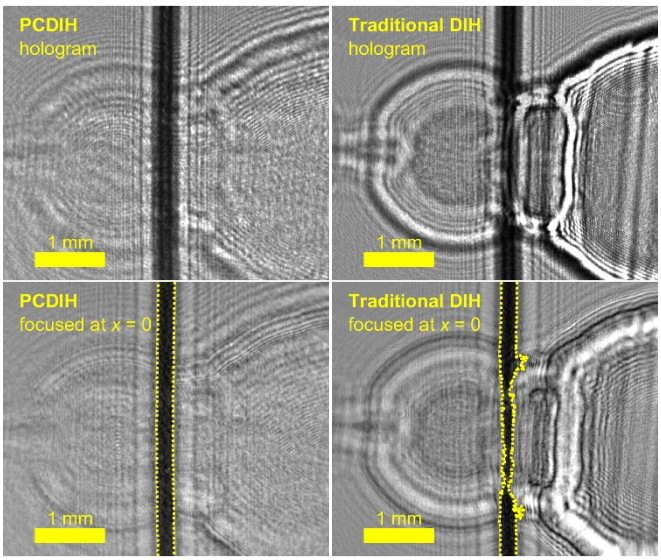

Fig. 4. (top) Holograms of a stationary wire imaged through a laser spark at x = 15 mm. (bottom) Results after numerically refocusing to x = 0. PCDIH results in (a) recover a high-quality image of the wire, while traditional DIH images in (b) are severely distorted by the index-of-refraction gradients.

Operation can be understood by returning to Fig 2. As the beam passes from left to right over the wire, a portion is absorbed and reflected, forming what is commonly referred to as the object beam, while the remaining collimated light forms a reference beam. Next, the phase of the object and reference beams is altered by the laser spark. These distorted beams then propagate an additional 46 mm to the DIH image plane where interference produces the results shown in Fig 4b.

In PCDIH, the object and reference beams, including phase distortions, are conjugated at the PC mirror and propagate back in the negative *x*-direction. The conjugate distortions are then canceled after passing back through the laser spark resulting in restored object and reference beams at $x = 15$ mm. At $x = 0$ these beams interfere to form a real image of the wire coincident with the actual wire. Finally, further propagation to the PCDIH image plane produces the results shown in Fig 4a. Note, this method would not work if the object was solely a phase distortion. In addition, semi-translucent objects would likely appear darker due to double passing of abortive features.

The ability to fully correct phase distortions is a function of the position of the distortion with respect to the object. For example, Fig 5 shows results when the laser spark is located at $x = -15$ mm. Notice how much, but not all, of the apparent distortion is removed in the PCDIH result. It is also noteworthy that Fig 5a shows better image quality compared to the equivalent DIH experiment with the disturbance after the object, Fig 4b. In this case, the distortions are not completely removed when the conjugate beams interact with the wire for the second time. Therefore, the object beam is expected to be only partially restored. Still, the conjugate reference beam, which does not interact with the object, is restored to a planar wave after passing back through the disturbance at $x = -15$ mm. Therefore, with the distortion located after the object, PCDIH restores the reference beam but only partially corrects the object beam. This is believed to be why PCDIH (Fig 5a) outperforms DIH (Fig 4b), but does not achieve perfect reconstruction.

Performance is quantified by recording 500 simultaneous DIH and PCDIH images at all conditions listed in Table 1. Each image is processed to automatically measure the apparent wire edges, with example results shown by the dotted yellow lines in Figs 4 and 5.

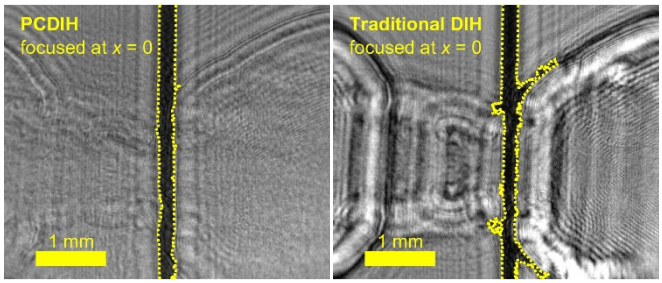

(a) (b)

Fig. 5. A stationary wire imaged through a laser spark at $x = -15$ mm. Images are numerically refocused to the optical depth of the wire. PCDIH data (a) can be refocused to recover a high-quality image of the wire, while traditional DIH results (b) are severely distorted by the index-of-refraction gradients.

Table 1. Standard deviation of the measured apparent location of the wire edges in μm as a function of the laser spark location. Results are from 500 images at each condition.

	no spark	$x = 15$ mm	$x = -15$ mm
DIH	0.6	69	140
PCDIH	1.9	8.2	12

Finally, results in Table 1 show the standard deviations of wire position for all frames averaged over the length of the wire. In the absence of any distortion (second column) both the DIH and PCDIH results show small shot-to-shot variations, roughly equal to the effective pixel size (1.9 μm). In contrast, when distorted by the laser spark, PCDIH consistently shows an order of magnitude better performance compared to traditional DIH. Furthermore, the best overall PCDIH performance is obtained when the laser spark is at $x = 15$ mm for the reasons previously mentioned.

The PCDIH results in Fig 4 and 5 appear to show much weaker intensity variations caused by the shock, although, interestingly, some effects remain. In theory, an ideal PC imaging configuration would completely remove the effects of a pure phase disturbance. Here, the phase disturbance is created by a shock wave traveling at least Mach one conditions (>300 m/s) which moves ~0.6 μm during the ~2 ns roundtrip time to the PC mirror and back. It is possible that this motion prevents complete correction of the phase disturbance. Alternatively, it is possible that very near the shock the temperature and pressure are sufficiently high to create significant absorption in the air with effects amplified by the double pass PCDIH configuration.

Figure 6 shows the results when the holograms in Fig 4 are numerically refocused to the location of the laser spark. Compared with Fig 4b, the image of the shock in Fig 6b might be slightly better focused, although large intensity variations remain making interpretation of any shock structure nearly impossible. This is perhaps why, to our knowledge, traditional DIH has never been used for quantitative 3D investigation of shock structure. In contrast, the refocused PCDIH result in Fig 6a appears to much more clearly show the edge of the shock with perhaps sufficient depth resolution to enable 3D measurements. More work is needed to better understand the true source of this signal. Nevertheless, these results hint at another potential application of the proposed PCDIH configuration.

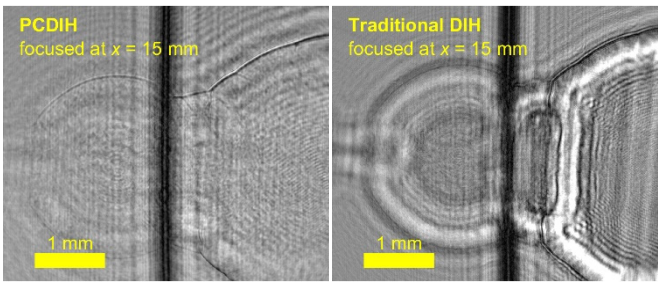

(a) (b)

Fig. 6. Results after holograms in Fig 4 are numerically refocused to the optical depth of the laser spark. In the traditional DIH images in (b) the expected shock structure is convoluted with large intensity variations likely originating from phase disturbances in the post-shock regions. In contrast, the PCDIH results in (a) appears to eliminate these issues.

Finally, experiments are performed using the configuration shown in Fig 2 wherein the wire and laser spark are substituted with explosively generated, hypervelocity metal fragments. Fig 1 shows the traditional DIH results. As already mentioned, images of downstream particles are highly distorted by gas-phase shock waves generated by particle motion at over 2 km/s [4]. In contrast, the simultaneously recorded PCDIH results in Fig 7 show significant improvement in the resolution of downstream particles. Note, in this application conical shock waves surround each particle; therefore, these results provide further evidence that PCDIH improves image quality even when distortions are located on both sides of the objects. Finally, the shape and 3D position of all particles in the field of view are quantified as shown in Fig 7c. This was not possible in the previous DIH investigation of this flow [4].

This work uses a regeneratively amplified ps laser and BEFWM to produce the PC signal. This was chosen due to the laser's high beam quality as well as literature which indicates that BEFWM may produce a higher fidelity PC signal compared to alternative methods such as SBS [12]. Nevertheless, for future applications complexity may be significantly reduced using injection seeded ns lasers to generate BEFWM with a single pump that is retroreflected off a normal incidence mirror or by eliminating the pumps altogether and focusing with sufficient energy to generate SBS. Both configurations are explored in an initial conference proceeding where successful PCDIH is reported, although more work is needed to study experimental tradeoffs [13].

In addition, further investigation is needed to better understand the limitations of the PCDIH technique and those applications where it is best suited. As already mentioned, the ability to correct distortions is expected to be a function of the position of the disturbance with respect to the object. Furthermore, in [13] performance is also shown to depend on the nature of the disturbance. For example, a disturbance which translates the beam between the object and the PCDIH image plane is not removed.

In summary, this letter proposes a phase conjugate digital inline holography (PCDIH) configuration for quantitative, 3D imaging of absorptive objects in measurement volumes containing phase disturbances which otherwise obscure traditional digital inline holography (DIH). Results are presented which quantify an order of magnitude improvement in object reconstruction when a stationary wire is imaged through a laser spark. Furthermore, application to explosively generated hypervelocity metal fragments shows a dramatic improvement in image quality for PCDIH (Fig 7) compared to traditional DIH (Fig 1). These results extend the application space for 3D holography to challenging environments which impart rapidly varying phase distortions.

Funding. U.S. Department of Energy (DE-NA0003525)

Acknowledgment. The authors gratefully acknowledge Lee Stauffacher and Jeff Heyborne for assisting with the experiments shown in Fig 1 and 7 and Seth Spitzer for assistance with initial setup. All are from Sandia National Laboratories. This work was supported by the Laboratory Directed Research and Development (LDRD) program at Sandia National Laboratories, which is a multi-mission laboratory managed and operated by National Technology and Engineering Solutions of Sandia, LLC., a wholly owned subsidiary of Honeywell International, Inc., for the U.S. Department of Energy's National Nuclear Security Administration under contract DE-NA0003525.

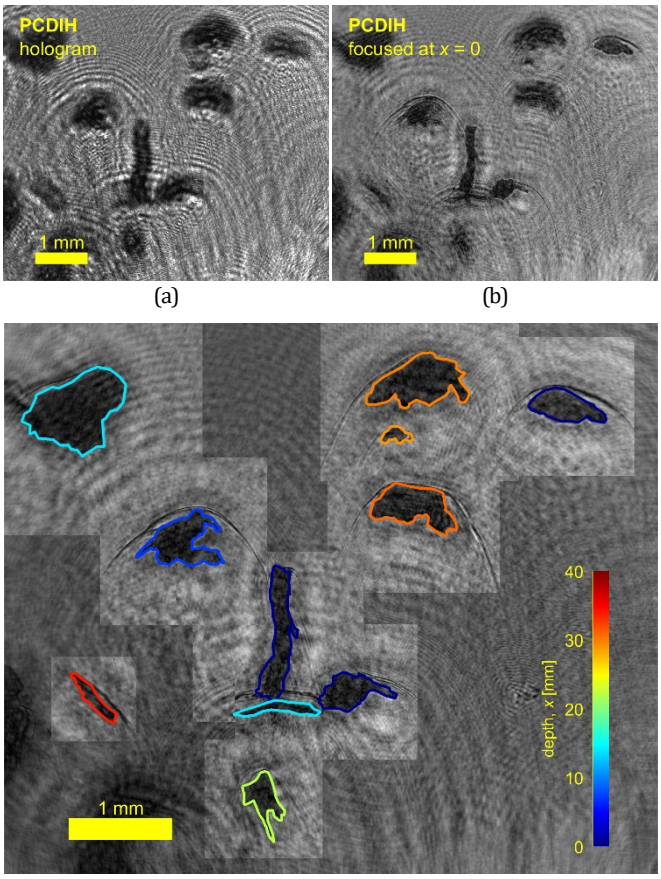

Fig. 7. PCDIH results of hypervelocity metal particles traveling from bottom to top, recorded simultaneous with the traditional DIH results in Fig 1. Diffraction patterns from individual particles are easily recognized in the hologram in (a) and are refocused in (b). The 3D results in (c) show bright squares refocused to the optical depth of each particle as indicated by the color outlines.

References

1. J. Katz and J. Sheng, Annu. Rev. Fluid Mech. **42**, 531 (2010).
2. N. A. Buchmann, C. Atkinson, and J. Soria, Meas. Sci. Technol. **24**, 024005 (2013).
3. D. R. Guildenbecher, J. Gao, P. L. Reu, and J. Chen, Appl. Opt. **52**, 3790 (2013).
4. J. D. Yeager, P. R. Bowden, D. R. Guildenbecher, and J. D. Olles, J. Appl. Phys. **122** (2017).
5. G. S. He, Prog. Quant. Electron. **26**, 131 (2002).
6. O. V. Kulagin, G. A. Pasmanik, and A. A. Shilov, Sov. Phys. Uspekhi **35**, 506 (1992).
7. H. Kogelnik, Bell Syst. Tech. J. **44**, 2451 (1965).
8. D. M. Bloom and G. C. Bjorklund, Appl. Phys. Lett. **31**, 592 (1977).
9. X. Zou, P. Zhao, P. Hong, X. Lin, Y. J. Ding, X. Mu, H.-C. Lee, S. K. Meissner, and H. Meissner, Opt. Lett. **38**, 3054 (2013).
10. L. Büttner, C. Leithold, and J. Czarske, Opt. Express **21**, 30653 (2013).
11. H. Yoshida, V. Kmetik, H. Fujita, M. Nakatsuka, T. Yamanaka, and K. Yoshida, Appl. Opt. **36**, 3739 (1997).
12. D. H. Beak, J. W. Yoon, J. S. Shin, and H. J. Kong, Appl. Phys. Lett. **93**, 231113 (2008).
13. K. N. G. Hoffmeister, S. P. Kearney, and D. R. Guildenbecher, *in 54th AIAA Aerospace Sciences Meeting 2016*